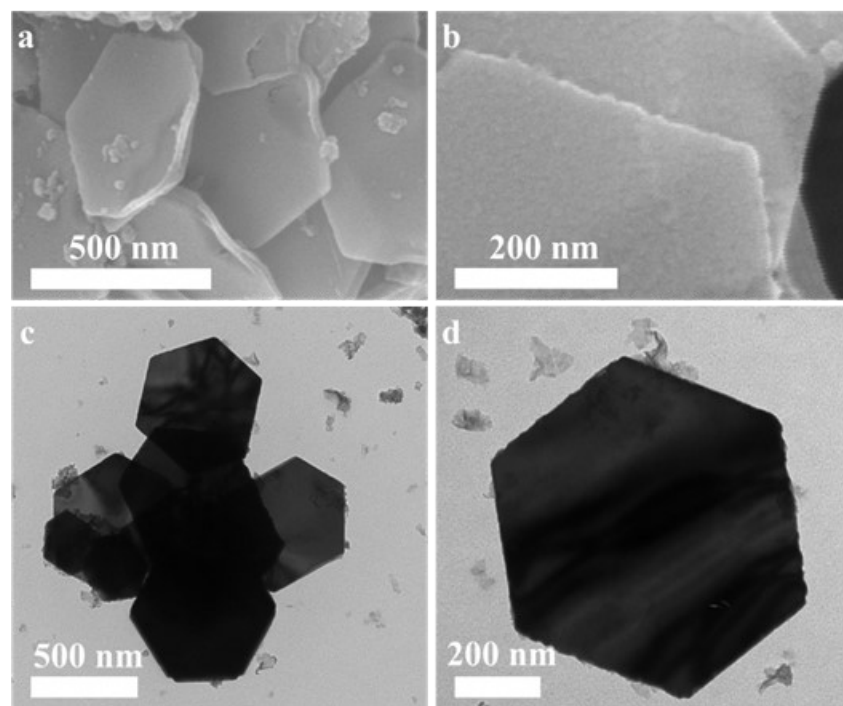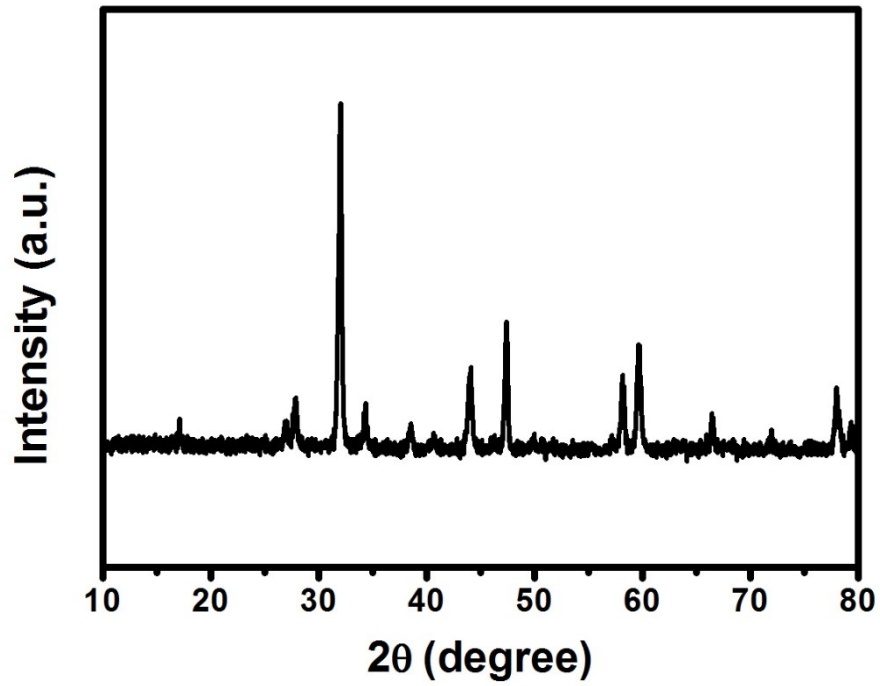**Pseudocapacitance-boosted ultrafast and stable Na-storage in NiTe$_2$ coupled with N-Doped carbon nanosheets for advanced sodium-ion half/full batteries**

Xu Han[a], Qilei Jiang[a], Mengling Zhang[a], Zheng Qin[a], Hongbo Geng*[b], Chencheng Sun*[c], Hongwei Gu*[a]

Figure S1. The microstructure and morphology of NiTe$_2$/PDA. (a-b) SEM images; (c-d) TEM images

Figure S2. The XRD diagram of the product after the solvothermal reaction. We performed XRD analysis of the products after the solvothermal reaction, and the results showed that the product obtained was $NiTe_2$ crystals (JCPDS NO. 89-2642).
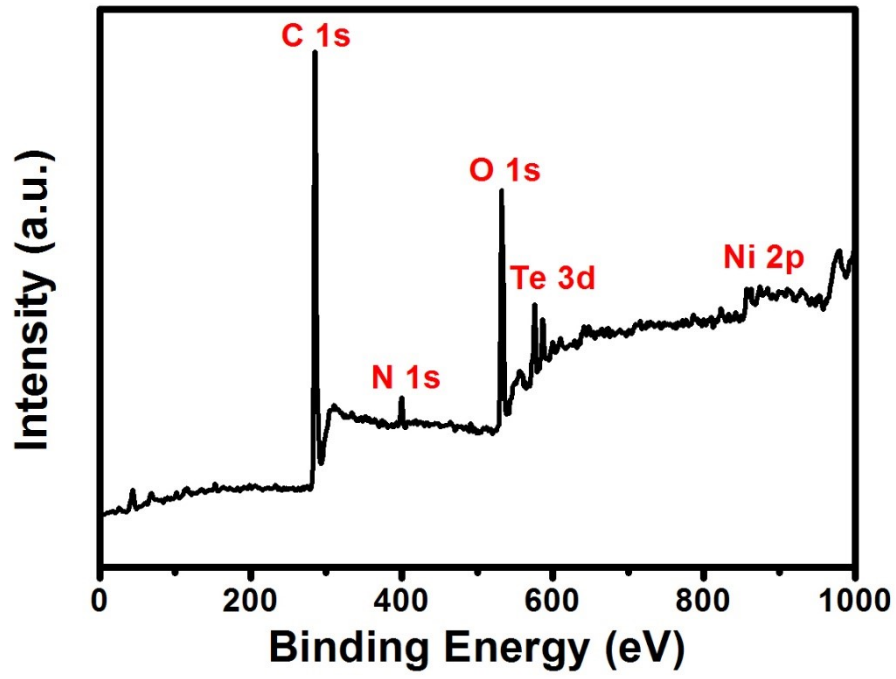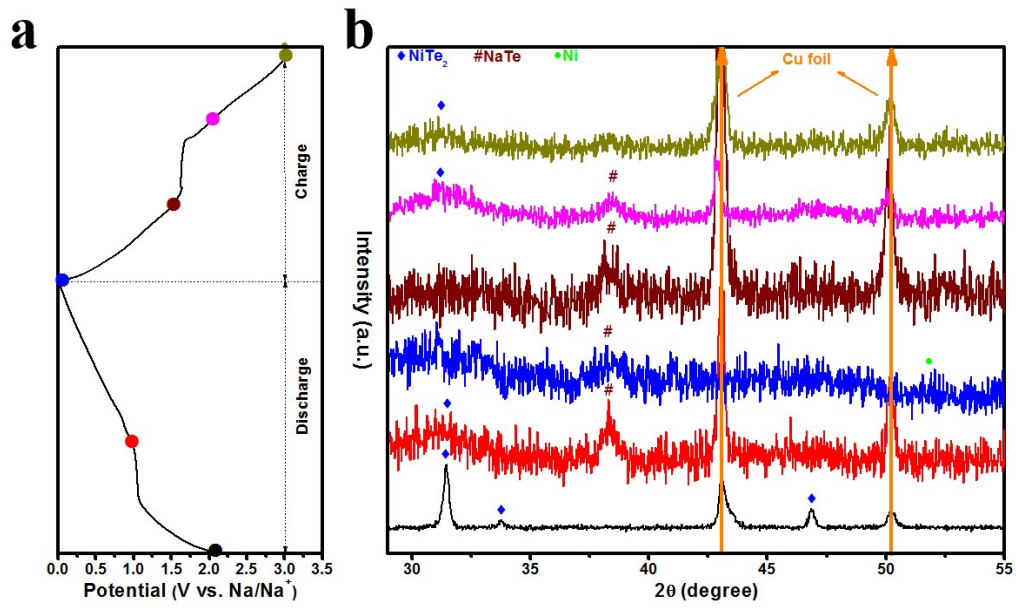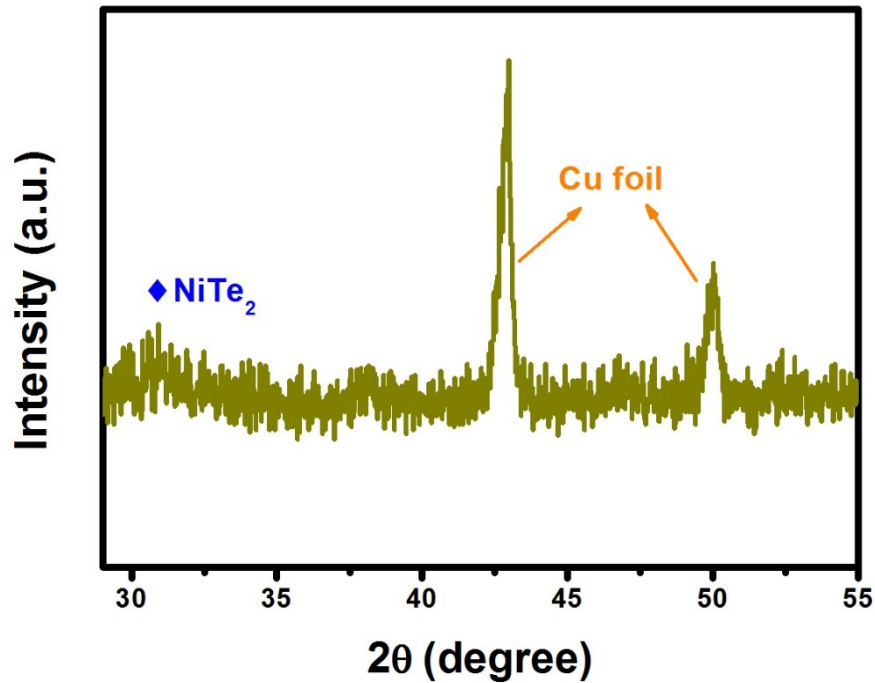
**Figure S3.** The XPS survey spectrum of the NiTe$_2$/NC.

Figure S4. Investigation of the electrochemical reaction mechanism of NiTe$_2$/NC for SIBs. (a, b) Typical GCD curves and cycle performance at 0.1 A g^{-1} and the *ex-situ* XRD patterns for the initial cycle.

Figure S5. The XRD pattern of electrode material at the first charge to 3.0V.

It was found that there was a weak peak at about 31.6° that could be indexed to the (011) crystal plane of NiTe$_2$ (JCPDS NO.89-2642). As NiTe$_2$ nanoparticles cannot recover to their original highly crystalline structure after charge and discharge resulting in weak peaks in the XRD patterns. This result explains the shift of the reduction peak to a high potential after the first cycle in the CV curves.[1, 2]
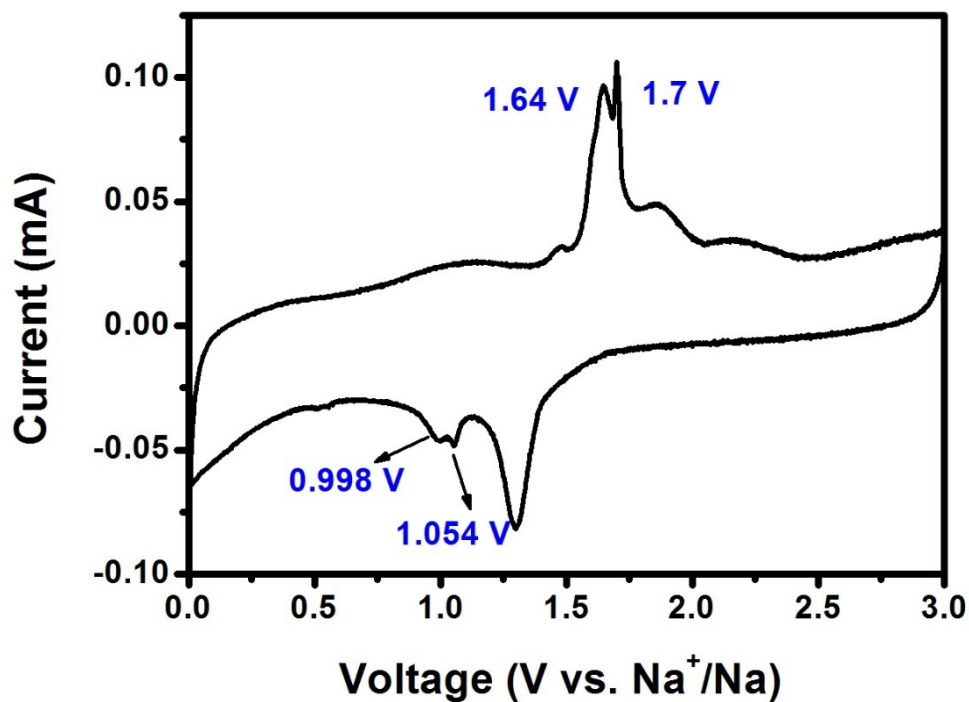
Figure S6. The third circle CV curve was collected at the scanning rate of 0.1mV s^{-1}.

According to previous reports, the reason for the occurrence of the oxidation peak at 1.7V is that some Na$_x$NiTe$_2$ cannot be completely deintercalation to form NiTe$_2$, leading to the split of the oxidation peak at 1.68V in the first circle into two oxidation peaks at 1.7V and 1.64V, which is also the reason for the attenuation of battery capacity.[3, 4] The wide peak at 2.2V is due to the gradual deintercalation of sodium ions in Na$_x$NiTe$_2$ nanocrystals, similar to the transition metal chalcogenides reported.
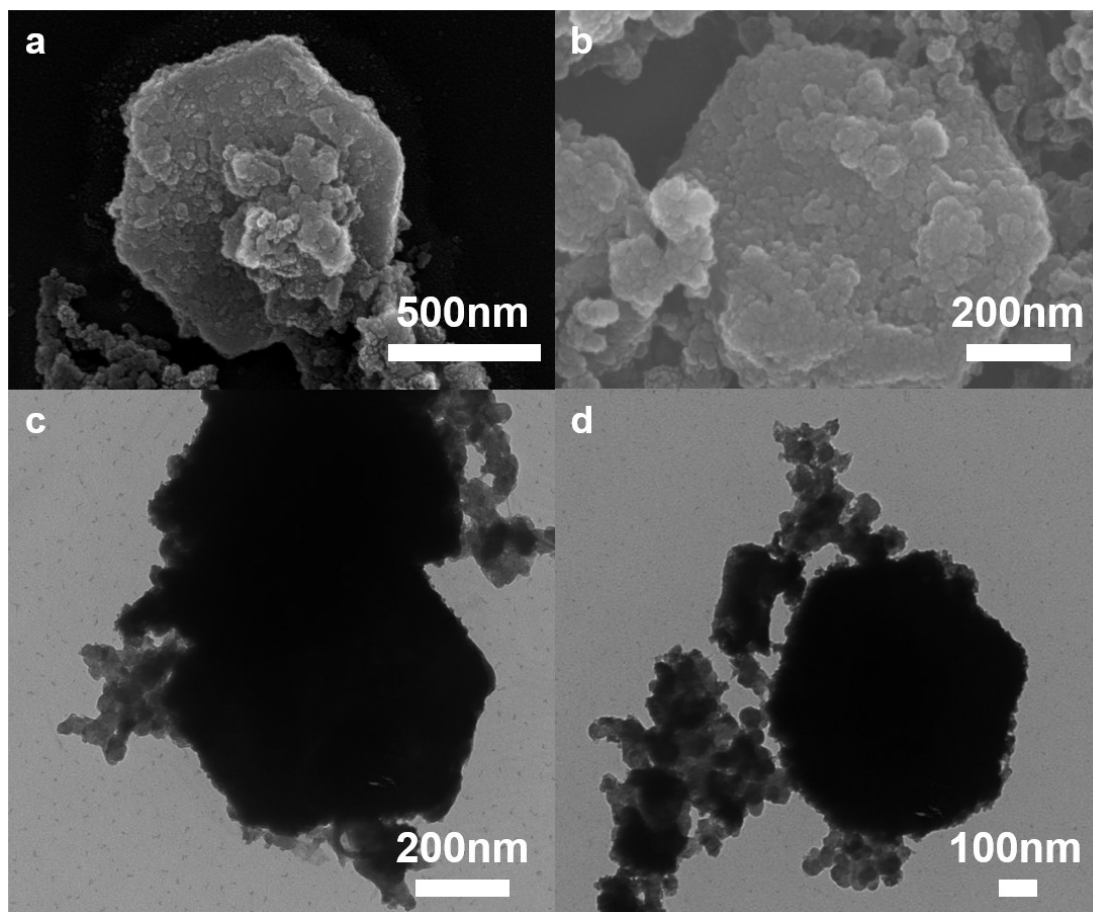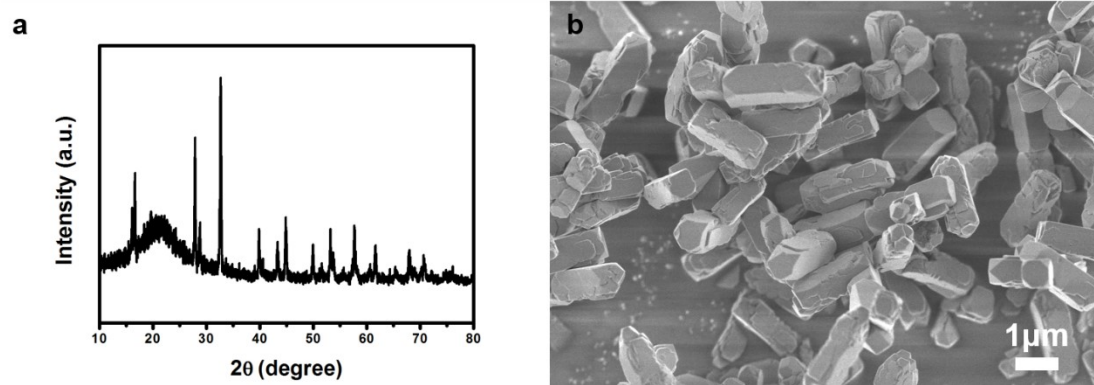
Figure S7. (a-b) SEM images; (c-d) TEM images of the NiTe$_2$/NC after cycling.
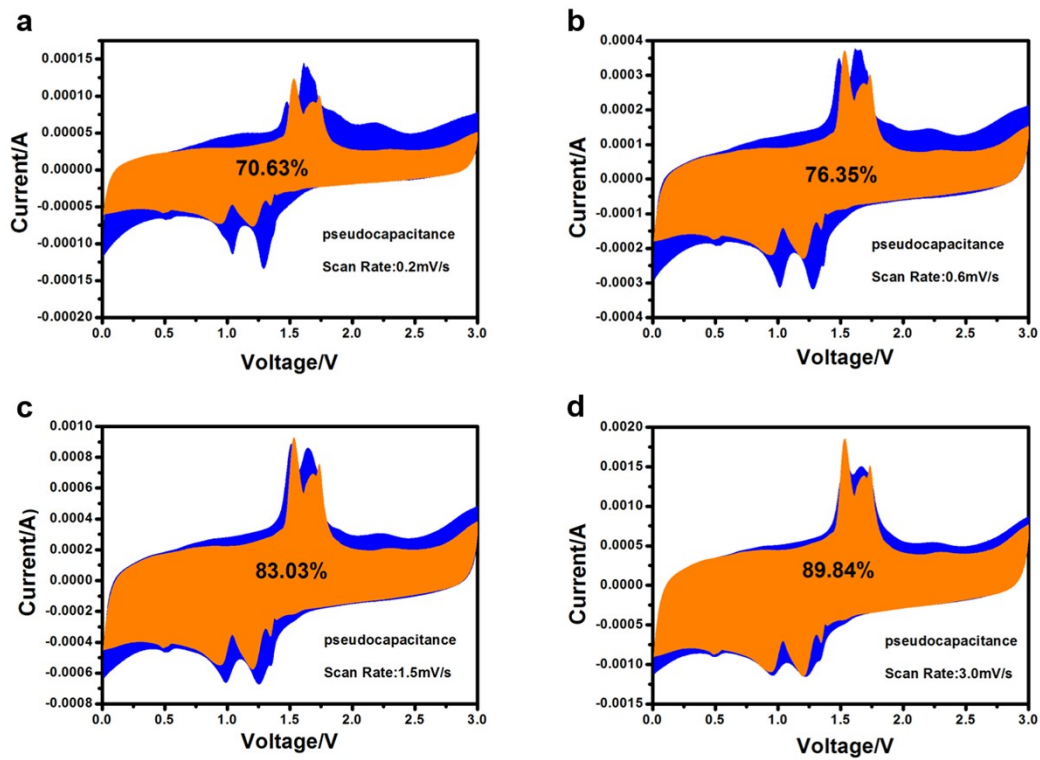
Figure S8. Capacitive contribution in CV curves under the scan rate of (a) 0.2, (b) 0.6, (c) 1.5 and (d) 3.0 mV s⁻¹.

Figure S9. (a) XRD pattern and (b) SEM image of $Na_3V_2(PO_4)_2O_2F$.

1. Y. Ding, W. Wang, M. Bi, J. Guo and Z. Fang, *Electrochim. Acta*, 2019, **313**, 331-340.
2. G. Zhang, K. Liu and J. Zhou, *J. Mater. Chem. A*, 2018, **6**, 6335-6343.
3. D. Sun, S. Liu, G. Zhang and J. Zhou, *Chem. Eng. J.*, 2019, **359**, 1659-1667.
4. X. Ou, J. Li, F. Zheng, P. Wu, Q. Pan, X. Xiong, C. Yang and M. Liu, *J. Power Sources*, 2017, **343**, 483-491.